Two-Dimensional Kinematics of Horses at Trot Through Videiomatry and Mathematical Modeling

Cinemática 2D de caballos al trote mediante videometría y modelamiento matemático

Cinemática 2D de cavalos ao trote mediante videometria e modelamento matemático

Yolanda Torres-Pérez*
Edwin Yesid Gómez-Pachón**
Francisco Miró-Rodríguez***

Fecha de recepción: 13 de junio de 2016
Fecha de aprobación: 10 de abril de 2017

Abstract

Currently, the direct observation method is used to assess the movement of horses; however, this method is limited, totally subjective, and many details of the musculoskeletal system functionality cannot be detected and evaluated because they are not perceptible to the naked eye. This study aimed at developing a mathematical model that calculates, plots, and simulates the 2D angular movement of some horse joints. The horse musculoskeletal system was modeled as a mechanical system of rigid bodies articulated by 15 simple joints. The mathematical solution of the mechanism was obtained from the standpoint of inverse kinematics (flat) liabilities. We constructed 15 link equations, associating the body segments of the system in movement with an inertia base, and used the mathematical optimization method based on the least squares calculation. We obtained kinematic curves of the main joints, as well as the trajectories (height) of the markers on fore and hind coronary band (hoofs), and a simulation of the mechanical system. This tool removes subjectivity and enables veterinarians to observe, evaluate (qualitatively and quantitatively), diagnose, and investigate different phenomena of the horse gait.

Keywords: Angular kinematics; Horse locomotion; Inverse kinematics; Mathematical model; Videometry.

Resumen

Actualmente, el método de observación directa se utiliza para evaluar el movimiento de los caballos; sin embargo, este método es limitado dado que es totalmente subjetivo y muchos detalles de la funcionalidad del sistema músculo-esquelético no pueden ser detectados y evaluados, debido a que no son perceptibles a simple vista. El principal objetivo de este estudio fue desarrollar un modelo matemático que permita calcular, graficar y simular el movimiento angular, en dos dimensiones, de algunas articulaciones de los caballos. El aparato locomotor del caballo fue modelado como un sistema mecánico de cuerpos rígidos articulados por 15 juntas simples. La solución matemática del mecanismo se hizo desde el punto de vista del pasivo de la cinemática inversa (plana); se

* Ph. D. Universidad Santo Tomás (Tunja-Boyacá, Colombia). yolanda.torres@usantoto.edu.co. ORCID: 0000-0002-3526-8491.
** Ph. D. Universidad Pedagógica y Tecnológica de Colombia (Tunja-Boyacá, Colombia). edwin.gomez02@uptc.edu.co. ORCID: 0000-0002-2733-5252.
*** Ph. D. Universidad de Córdoba (Córdoba, España). an1mirof@uco.es. ORCID: 0000-0001-7629-0057.

construyeron 15 ecuaciones de cadena, asociando los segmentos corporales del sistema en movimiento con la base inercial, y fue utilizado el método de optimización matemática basada en el cálculo de los mínimos cuadrados.

En este estudio se obtuvieron las curvas cinemáticas de las principales articulaciones, las trayectorias (altura) de los marcadores sobre las bandas coronarias trasera y delantera (cascos) y una simulación del sistema mecánico. Esta herramienta elimina la subjetividad y permite a los veterinarios observar, evaluar (cualitativa y cuantitativamente), diagnosticar e investigar sobre diferentes fenómenos de la marcha de los caballos.

Palabras clave: Cinemática angular; Cinemática inversa; Marcha quina; Modelo matemático; Videometría.

Resumo

Atualmente, o método de observação direta utiliza-se para avaliar o movimento dos cavalos; porém, este método é limitado já que é totalmente subjetivo e muitos detalhes da funcionalidade do sistema músculo-esquelético não podem ser detectados e avaliados, devido a que não são perceptíveis a olho nu. O principal objetivo deste estudo foi desenvolver um modelo matemático que permita calcular, plotar e simular o movimento angular, em duas dimensões, de algumas articulações dos cavalos. O aparelho locomotor do cavalo foi modelado como um sistema mecânico de corpos rígidos articulados por 15 juntas simples. A solução matemática do mecanismo fez-se desde o ponto de vista do passivo da cinemática inversa (plana); construíram-se 15 equações de cadeia, associando os segmentos corporais do sistema em movimento com a base inercial, e foi utilizado o método de otimização matemática baseada no cálculo dos mínimos quadrados.

Neste estudo obtiveram-se as curvas cinemáticas das principais articulações, as trajetórias (altura) dos marcadores sobre as bandas coronárias traseira e dianteira (cascos) e uma simulação do sistema mecânico. Esta ferramenta elimina a subjetividade e permite aos veterinários observar, avaliar (qualitativa e quantitativamente), diagnosticar e pesquisar sobre diferentes fenômenos da marcha dos cavalos.

Palavras chave: Cinemática angular; Cinemática inversa; Marcha equina; Modelo matemático; Videometria.

Cómo citar este artículo:
Y. Torres-Pérez, E. Y. Gómez-Pachón, and F. Miró-Rodríguez, "Two-Dimensional kinematics of horses at trot through videometry and mathematical modeling," *Rev. Fac. Ing.*, vol. 26 (45), pp. 83-96, May. 2017.

I. Introduction

Although some of the horse morphological and locomotion characteristics can be perceived by the trained eye of an expert, the direct observation method lacks any quantitative and objective validity because it depends on the expertise, training, and judgment of each veterinarian. Moreover, several important aspects of the musculoskeletal system functionality, and the kinematic joint cannot be evaluated.

For horse motion analysis, different techniques, such as analytical photogrammetry [1], videometry [2], accelerometry [3], electromyography [4], and, rarely, mathematical modeling [5-7] have been used to help veterinarians and researchers to quantify movement. The first two techniques have several advantages, one of them is that the horse's body does not have to be instrumented and wired, and other is that they allow a qualitative and quantitative analysis of the horse gait. On the other hand, with accelerometers and electromyography is almost mandatory to instrument the animal, and the obtained results are mathematical values or electrical signals, which require a more complex processing for their interpretation. These techniques have proven to be useful for assessing the horse conformation [8], analyzing the gait in different breeds (Pure Spanish [9] Andalusian [10], Angloarabian, Warmblood [4], and others [11]), determining the characteristics of movement at hand-led walk [2, 9] and at different types of trot [12], analyzing the influence of speed and height on the withers [13], and studying the effect of different surfaces [14].

To our knowledge, there are few studies on mathematical modeling of equine movement, which allows different kinematic [5, 15-16] and kinetic calculations [6, 19]. Some of the most relevant studies are based on 2D or 3D kinematics analysis of the interphalangeal [15] and metacarpophalangeal joints [16]; in these studies, the authors only obtained ranges of motion for flexion/extension, adduction/abduction, and internal/external rotation at walk and at trot. Furthermore, other authors have simulated the horse motion as a series of rigid articulated bodies [17-18], and have used coordinate systems for quantifying movements of the horse's digital joint [7], allowing a better evaluation of the kinematic and kinetic of all horse joints. In these studies, horse articular movement is very useful for characterizing its locomotion patterns, and for understanding its etiology, injury evolution and treatment, progress of training programs, etc.

The objectives of this study were to develop a mathematical model to generate and evaluate, qualitatively and quantitatively, the motion kinematics graphs of the most important horse joints, simulate the motion pattern for the fore and hind limbs, and, ultimately, assist scientists and veterinarians in an objective assessment of equine movement.

The main contribution of this paper is the construction of a mathematical model that is able to generate trajectory and kinematic curves of multiple horse joints, and to facilitate numerical comparisons of each horse curve, at each percentage of the gait cycle, with the normality band with ± standard deviation. Also, the user can display a 2D representation of the kinematics chain of the horse skeleton in his anterior portion, posterior portion, or entire skeleton, which will allow the user to better understand the phenomenon of the equine gait, and will eliminate the subjectivity of horse movement evaluations and diagnoses. This will let veterinarians to assess, diagnose, rehabilitate, and monitor the equine gait in a more objective, accurate, and scientific manner.

This paper is divided as follows: the first section explains the methodology to construct the mathematical model of joint kinematics of any horse, and its posterior validation; the second section presents the main results; and the final section closes with the main conclusions.

II. Material and methods

A. Study subjects

Using computer-assisted videometry [9, 19-20], we obtained the average values (x and y coordinates) of the movement of markers placed on skeletal references of 25 Andalusian horses at trot (Fig. 1).

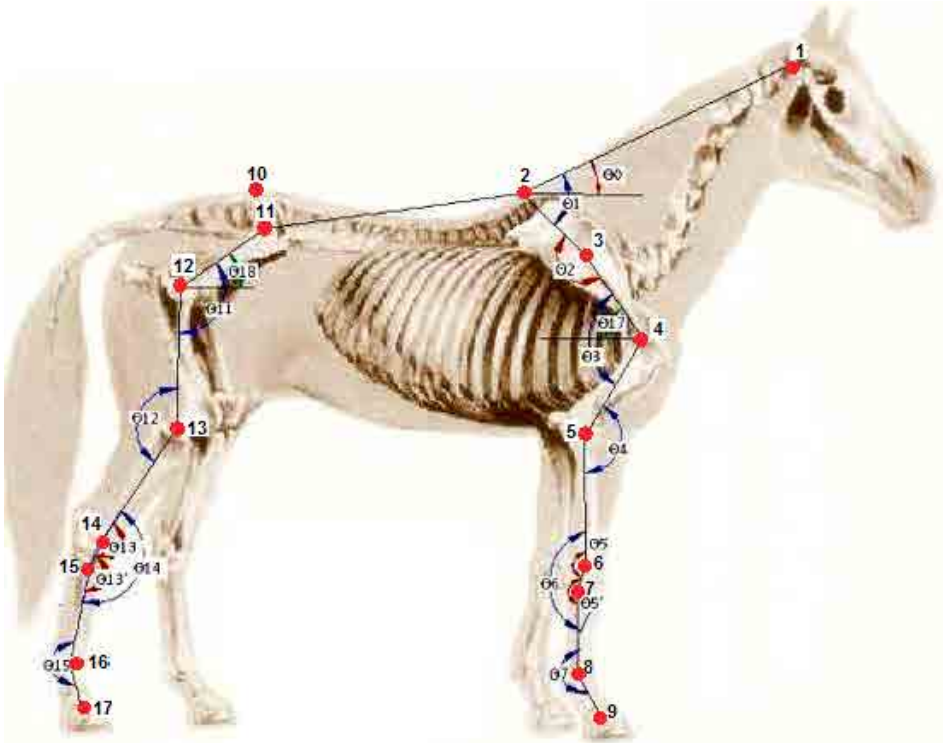

Fig. 1 Skeletal references (markers): 1. Wing of the atlas, 2. Withers, 3. Tuber of spina scapulae, 4. Greater tubercle of the humerus (caudal part), 5. Lateral collateral ligament of the elbow joint, 6. Lateral styloid process of the radius, 7. Proximal end of the metacarpal bone IV, 8. Lateral collateral ligament of the fore-fetlock joint, 9. Coronary band (forelimb), 10. Sacral tuber, 11. Coxal tuber, 12. Greater trochanter of the femur (caudal part), 13. Lateral collateral ligament of the stifle joint, 14. Lateral malleolus of the tibia, 15. Proximal end of the metatarsal bone IV, 16. Lateral collateral ligament of the hind fetlock joint, and 17. Coronary band (hind limb).

Figure 1 also shows the schematic representation of calculated joint angles. Angular variables are the following: θ0 (neck inclination), θ1 (neck angle), θ2 (scapular alignment), θ3 (shoulder), θ4 (elbow), θ5 (angle of radio vs. carpus), θ5' (carpal angle vs. metacarpus), θ6 (carpal angle), θ7 (fore-fetlock), θ11 (hip), θ12 (stifle), θ13 (angle of tibia vs. tarsus), θ13' (tarsal angle vs. metatarsal), θ14 (hock), θ15 (hind fetlock), θ17 (scapular inclination), and θ18 (pelvic inclination).

B. Mathematical model approach

The mathematical model was set up representing the horse as a mechanical system of rigid bodies articulated by simple joints (Fig.1). The model was developed using an inverse kinematics analysis, which employs basic principles of the kinematics of rigid bodies (Fig. 2).

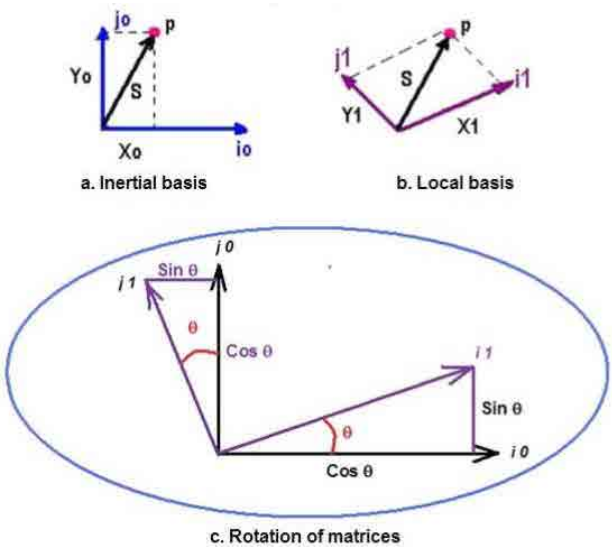

Fig. 2. Representation in the plane of a) inertia base, b) local base, and c) the rotation of matrices.

In the mathematical model, there is an external inertia base fixed on the origin (0,0), and there are 15 local mobile bases located in anatomical points (Fig. 3). These bases are rotated and move a distance (longitudinal to each segment) by means of inverse kinematics equations to calculate the angular movements.

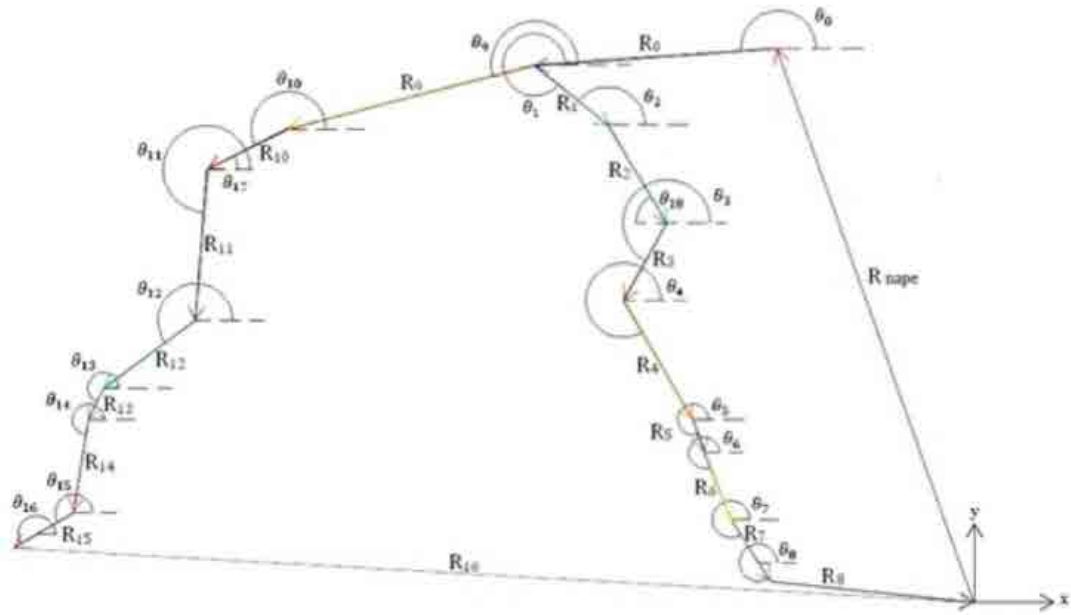

Fig. 3 Body segments vs. the horizontal axis angles and configuration of the vector array.

Figure 3 also shows the two main kinematics chains that represent the forelimb (Rnape+R0+R1+R2+R3+R4+R5+R6+R7) and the hind limb (Rnape+R0+R9+R10+R11+R12+R13+R14+R15), and that were used to calculate the inverse kinematics. The vectors, Rnape, R8, and R16 were used to complete the kinematics chains associated with fore and hind limbs, respectively.

Based on the representations shown in figure 2, the following correlations of the coordinates can be obtained:

$$S = x_0\, i_0 + y_0\, j_0 \tag{1}$$

$$x_0\, i_0 + y_0\, j_0 = x_1\, i_1 + y_1\, j_1 \tag{2}$$

$$i_1 = \cos\theta\, i_0 + \sin\theta\, j_0 \tag{3}$$

$$j_1 = -\sin\theta\, i_0 + \cos\theta\, j_0 \tag{4}$$

Thus, the general position equation is obtained.

$$R = [R_\theta]\, r \tag{5}$$

Where:

$$R = \begin{bmatrix} x_0 \\ y_0 \end{bmatrix} = [x_0 \quad y_0]^T \tag{6}$$

$$r = \begin{bmatrix} x_1 \\ y_1 \end{bmatrix} = [x_1 \quad y_1]^T \tag{7}$$

$$[R_\theta] = \begin{bmatrix} \cos\theta & -\sin\theta \\ \sin\theta & \cos\theta \end{bmatrix} \tag{8}$$

R[θ] is the rotation matrix.

The position of the mechanism was analyzed from a passive point of view, with a coordinate system having an inertia base fixed to the ground (external), and mobile local bases located on the skeletal references, united to the joints of the mechanism (aligned in X) (Fig.3), for which, a related base change matrix was built (8) [21]. The vectors employed for this biomechanical system are presented in Table 1.

Table 1

Mathematical proposal for the vectors of the fore and hind limbs employed in the mathematical model (ri are the lengths of the segments)

Anterior Section	Posterior Section
$R_{nape} = \{x_{nu}, y_{nu}\}$	
$R_{withers} = \{x_{withers}, y_{withers}\}$	
$R_0 = R[q_0] \cdot r_0$	$R_9 = R[q_9] \cdot r_9$
$R_1 = R[q_1] \cdot r_1$	$R_{10} = R[q_{10}] \cdot r_{10}$
$R_2 = R[q_2] \cdot r_2$	$R_{11} = R[q_{11}] \cdot r_{11}$
$R_3 = R[q_3] \cdot r_3$	$R_{12} = R[q_{12}] \cdot r_{12}$
$R_4 = R[q_4] \cdot r_4$	$R_{13} = R[q_{13}] \cdot r_{13}$
$R_5 = R[q_5] \cdot r_5$	$R_{14} = R[q_{14}] \cdot r_{14}$
$R_6 = R[q_6] \cdot r_6$	$R_{15} = R[q_{15}] \cdot r_{15}$
$R_7 = R[q_7] \cdot r_7$	$R_{16} = \{x_f, y_f\}$
$R_8 = \{x_{cor}, y_{cor}\}$	$R_{17} = \{x_{mp}, y_{mp}\}$
$R_m = \{x_m, y_m\}$	$R_{18} = \{x_{t2}, y_{t2}\}$
$R_{c1} = \{x_{c1}, y_{c1}\}$	$R_{19} = \{x_{t1}, y_{t1}\}$
$R_{c2} = \{x_{c2}, y_{c2}\}$	$R_{20} = \{x_r, y_r\}$
$R_{co} = \{x_{co}, y_{co}\}$	$R_{21} = \{x_{ca}, y_{ca}\}$
$R_h = \{x_h, y_h\}$	$R_{22} = \{x_i, y_i\}$
$R_{es} = \{x_{es}, y_{es}\}$	

All vectors in Table 1 are related to each other to build the kinematics chains (Fig. 3), which, along with the rotation matrices, the vector magnitude, and the coordinates of each point, allow to calculate the angular movements by means of inverse kinematics.

C. Mathematical processing of information

- **Calculation of body segments length.** The length of the body segments (L0 – L15) was calculated using the coordinates (x, y) of each marker in the first frame of the stride of the experimental data, and using the equation (9) of distance between points.

$$d = \sqrt{(x_2 - x_1)^2 + (y_2 - y_1)^2} \quad (9)$$

- **Calculation of initial angles.** Markers on the skeletal references (Fig. 1) were used to define the angular variables of the system (at the initial time). These angles were calculated using the scalar product (10) and the coordinates (x, y) of the involved points 3 and 4 (Fig. 1), according to the protocol.

$$\overrightarrow{V_1}.\overrightarrow{V_2} = |V_1||V_2|\cos\alpha \quad (10)$$

- **Programming the mathematical model to calculate joint kinematics.** To calculate graphs and simulate the angular movements of each joint, we developed a script using the Mathematica® software, and incorporated the following items: the rotation matrices (8), the trajectory values (x, y coordinates) of each point throughout the gait

cycle, the lengths of each body segment, and the angles of each segment vs. the horizontal axis in frame 0 (initial frame of the gait cycle video), the mathematical approach of the vectors (Table 1), and the loop equations of each kinematics chain (11 - 25).

$$Pos = R_{nape} + R_0 + R_1 + R_2 + R_3 + R_4 + R_5 + R_6 + R_7 - R_8 \quad (11)$$

$$Pos_1 = R_m + R_7 - R_8 \quad (12)$$

$$Pos_2 = R_{c2} + R_6 + R_7 - R_8 \quad (13)$$

$$Pos_3 = R_{c1} + R_5 + R_6 + R_7 - R_8 \quad (14)$$

$$Pos_4 = R_{co} + R_4 + R_5 + R_6 + R_7 - R_8 \quad (15)$$

$$Pos_5 = R_h + R_3 + R_4 + R_5 + R_6 + R_7 - R_8 \quad (16)$$

$$Pos_6 = R_{es} + R_2 + R_3 + R_4 + R_5 + R_6 + R_7 - R_8 \quad (17)$$

$$Pos_7 = R_{withers} + R_1 + R_2 + R_3 + R_4 + R_5 + R_6 + R_7 - R_8 \quad (18)$$

$$Pos_8 = R_{nape} + R_0 + R_9 + R_{10} + R_{11} + R_{12} + R_{13} + R_{14} + R_{15} - R_{16} \quad (19)$$

$$Pos_9 = R_{22} + R_{10} + R_{11} + R_{12} + R_{13} + R_{14} + R_{15} - R_{16} \quad (20)$$

$$Pos_{10} = R_{21} + R_{11} + R_{12} + R_{13} + R_{14} + R_{15} - R_{16} \quad (21)$$

$$Pos_{11} = R_{20} + R_{12} + R_{13} + R_{14} + R_{15} - R_{16} \quad (22)$$

$$Pos_{12} = R_{19} + R_{13} + R_{14} + R_{15} - R_{16} \quad (23)$$

$$Pos_{13} = R_{18} + R_{14} + R_{15} - R_{16} \quad (24)$$

$$Pos_{14} = R_7 + R_{15} - R_{16} \quad (25)$$

- **Least Squares Method.** Because the system is nonlinear, with more unknowns than equations, a numerical analysis was performed using the mathematical optimization method created by Powell [22] and Fletcher [23], where, given a set of coordinates (x_k, y_k), where k = 1,2, ..., n., and f_j, with j = 1,2, ..., m, a basis of *m* functions, linearly independent, we found a function *f* linear combination of basic functions, such as f (xk) » yk, that is:

$$f(x) = \sum_{j=1}^{m} c_j f_j(x) \quad (26)$$

This method is measured and minimizes the error in the whole approach, making it necessary to find the *m* coefficients c_j that make the approximant function f(x) the best approximation to the points (x_k, y_k). The approximation process using the least square method (the steepest descent method) is based on the minimization of the mean square error (or equivalent), so we should minimize the filing of this error. The quadratic error is defined in (27).

$$E_c(f) = \frac{\sum_{K=1}^{n} (e_K)^2}{n} \quad (27)$$

For each loop equation (11-25), the function that best approximated the experimental data was calculated, according to the criterion of minimum square error (implemented in Mathematica®). With the sum of the objective functions

of each loop equation (28), a total objective function (29) was generated, which then was used to calculate the angular movement of the segments during the gait cycle.

$$fObjPos(i) = pos(i)[\![1]\!]^2 + pos(i)[\![2]\!]^2 \quad (28)$$

Where i = 0, 1, 2, ... , 14.

$$fObjTotal = fObjPos + fObjPos1 + fObjPos2 + fObjPos3 + \cdots + fObjPos14 \quad (29)$$

Posteriorly, to calculate and graph the variation in movement of the whole system of joint angles, we established correlations between angles; for example, the elbow joint angle was determined through equation (30) that correlated with the angles (not joints) q_4 and q_3.

$$\theta_{elbow} = \pi\text{-}(\theta_4\text{-}\theta_3) \quad (30)$$

D. Validation of the mathematical model results

We compared the results obtained by the mathematical model with those obtained by a Digital Video Morphometric System (DVMS) [9], for the same horses by the 2D videography analysis system. For every angular variable, the numerical difference between the experimental and the theoretical averages was determined for every 10 % of the motion cycle, and the average and standard deviation of these differences were calculated (Table 2). In addition, we visually inspected and compared the patterns graphs of the joint angle values vs. time (% stride), obtained by the mathematical model and those obtained by Digital Video Morphometric System (Fig 4).

Table 2

Average and standard deviation of the differences between the experimental average (videometry) and the theoretical average (mathematical model) for fore and hind limb angular variables

	Average (°)	Standard Deviation (°)
Neck Inclination	0.43	0.3
Scapular Inclination	1.57	0.68
Shoulder Kinematics	2.13	1.21
Elbow Kinematics	3.98	2.88
Carpal Kinematics	1.83	2.58
Fore Fetlock Kinematics	3.87	2.56
Fore Retraction – Protraction Angle	0.017	0.012
Height of the Fore Coronary Mark	0.0029	0.0024
Hip kinematics	4.3	2.44
Pelvic Inclination	1.8	0.61
Stifle Kinematics	5.78	5.3
Hock Kinematics	0.05	0.07
Hind Fetlock Kinematics	9.12	9.12
Hind Retraction – Protraction angle	0.02	0.01
Height of the Hind Coronary Mark	0.006	0.002

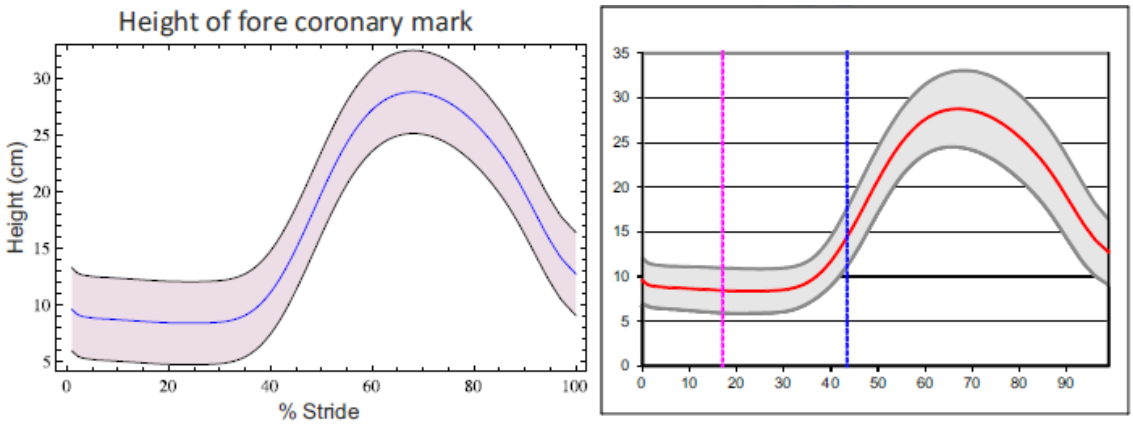

Fig. 4 Joint angle values vs. time (% stride); mathematical model (left) and experimentally (right).

III. Results

We designed a 2D-real-scale representation of an articulated rigid body system, with some of the most significant "body segments and joints", by means of the mathematical model. In addition, we obtained graphs of the joint angle values vs. time for the trajectories of the main markers (coordinates x, y).

For the 25 horses at trot, we generated graphs of the joint angle value vs. time for the angular variables of the fore and hind limbs (Fig. 5). Additionally, we calculated the standard deviation and maximum and minimum values of the angular variables for each angle. With these data, the software generated three normality bands (Fig. 6), which allowed us to make a quantitative and objective assessment of the equine locomotion pattern.

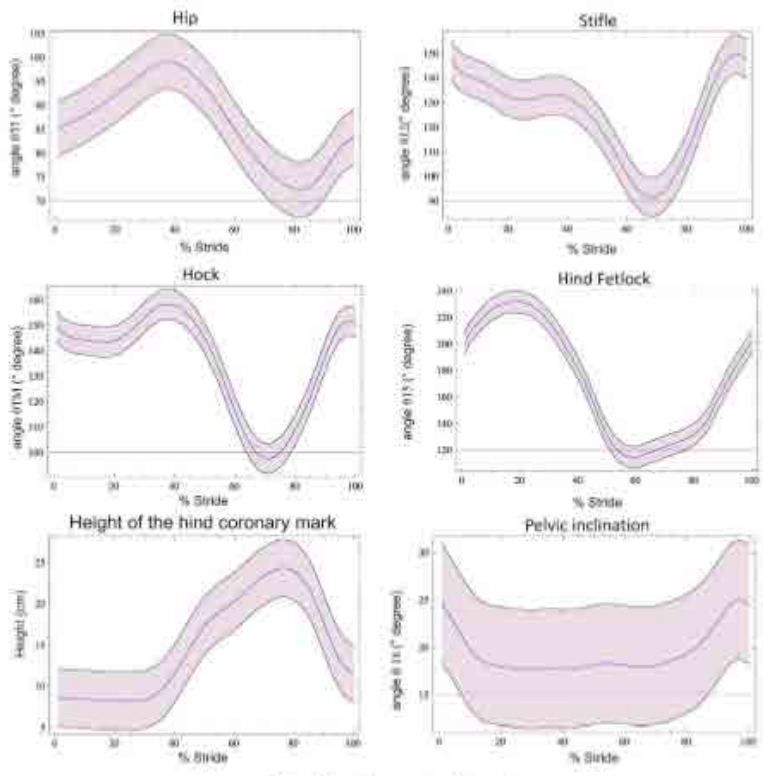

Fig. 5 Example of joint angles vs. time (% stride) graphs of hind limb (average ± standard deviation) for 25 horses at trot obtained by the mathematical model. Shadow areas are one standard deviation from the mean curves.

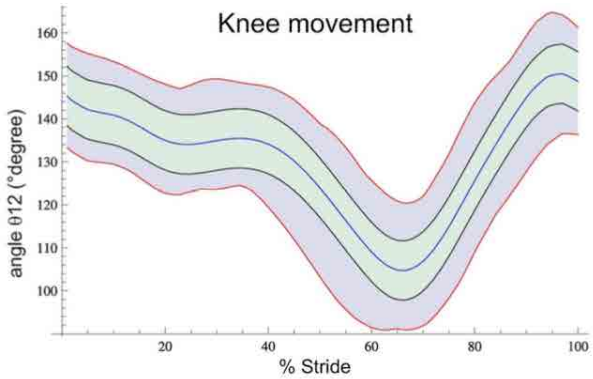

Fig. 6 Joint angles vs. time (% stride) graphs for the stifle (θ12) obtained by the mathematical model. Normality bands with mean values (blue line), ± standard deviation (black line), and ± minimum and maximum values (pink lines). The green zone represents the normality band.

For a better understanding of the equine movement, the fore and hind limb motion was simulated both separately and assembled (together), and displayed to the user (Fig. 7). During the simulation, the model allows to represent the trajectories of a specific, several, or all markers. It is also possible to check the normality or abnormality of the movement pattern through the full motion cycle.

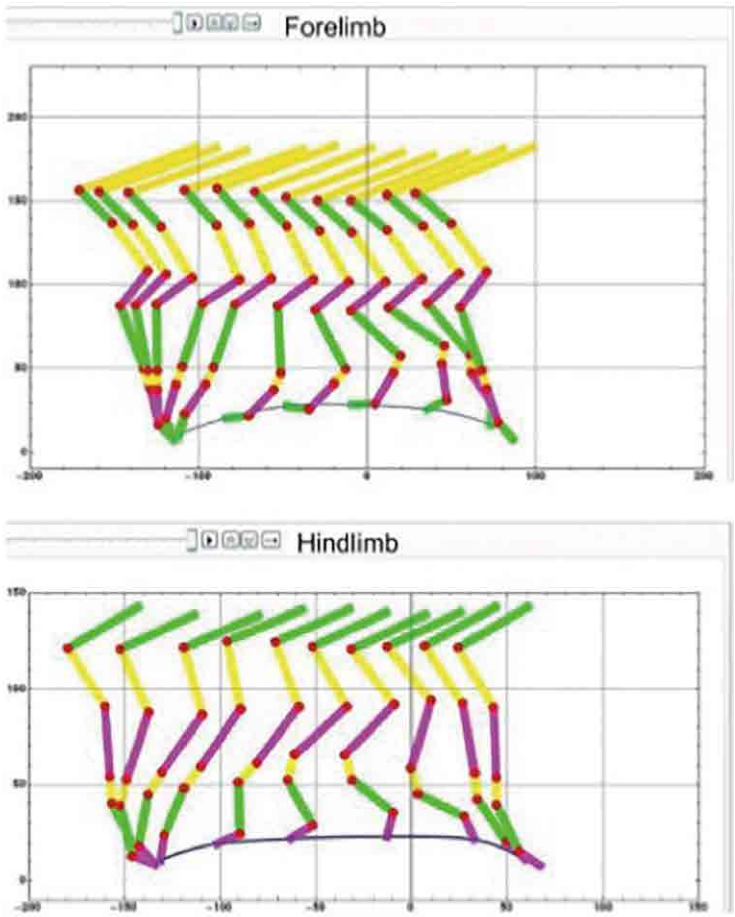

Fig. 7 Schematic representation of the simulation for fore (a) and hind (b) motion of a trotting horse (Sequences and trajectories of margo coronalis).

For every angular variable at every 10 % of the full motion cycle, the numerical difference between the experimental and the theoretical averages of each joint movement was calculated, and the results of this model were validated numerically and graphically.

The mathematical methodology used (kinematics chains), not only generated kinematics curves of the main joint variables (Fig. 4 and 5), but also created curves of other angular variables. The graphics obtained in this study could be helpful for future studies for analyzing normal and abnormal (lameness) equine movement.

In this study, we used the angles of the body segments with respect to the horizontal axis for the position equation (Fig. 3). For a better understanding of the graphical representation of the results, in which the traditional extension-flexion concept is maintained, it was necessary to make the conversions.

The numeric differences between the experimental (videometry) and the theoretical (mathematical model) averages were small, except for the hip (4.3°), the stifle (5.78°), and the hind fetlock (9.12°) joints. However, if these values are compared with the values for the full range of movement, the differences do not seem to be great (Table 2 and Fig. 4). Under visual inspection, the experimental and theoretical graphs were very similar in their starting values, and in their pattern shape (Fig. 8).

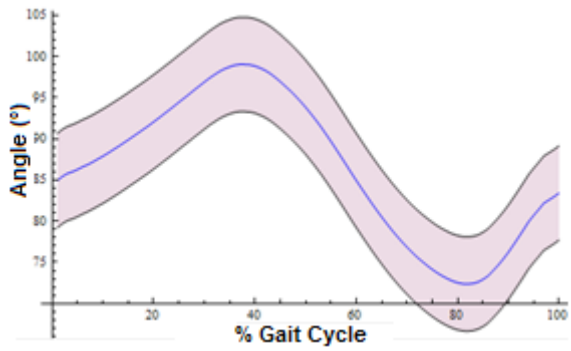

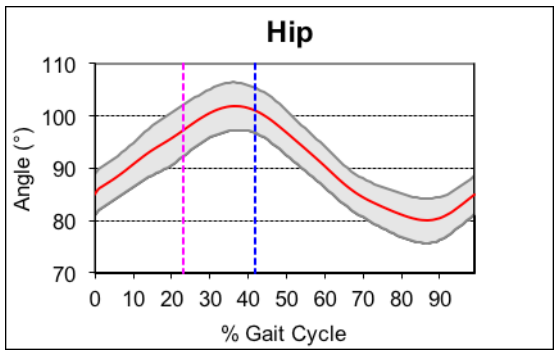

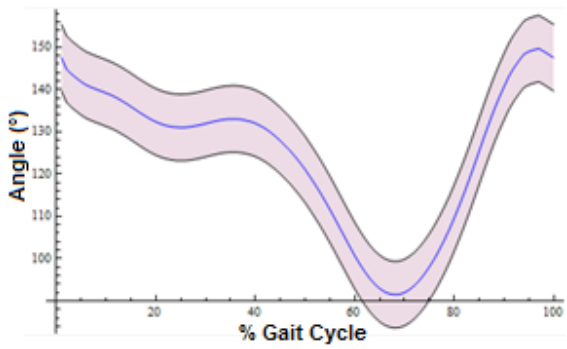

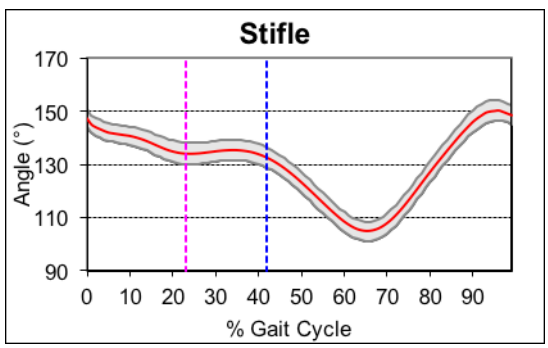

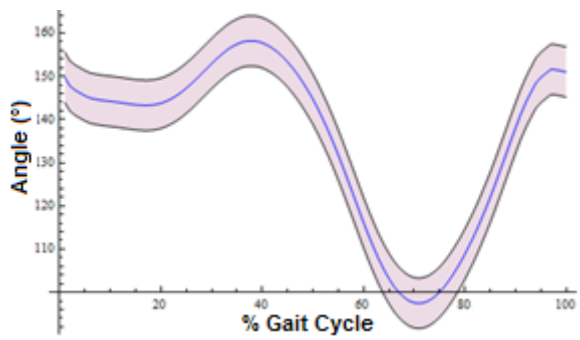

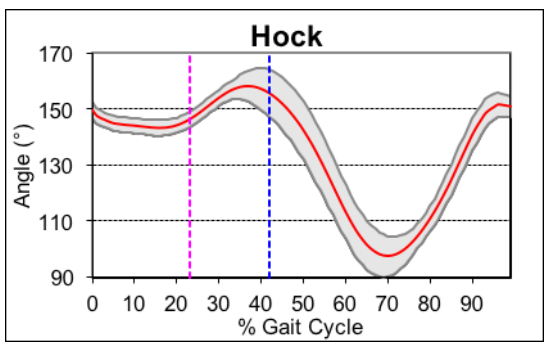

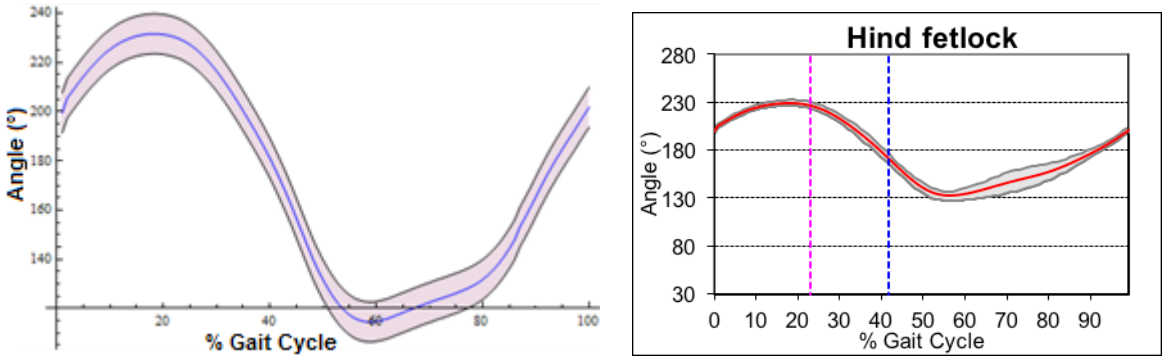

Fig. 8 Comparison between kinematics curves of the hind sections. Theoretical curves from the mathematical model (left column) and experimental curves from videometry (right column).

IV. Conclusions

Thanks to the mathematical model generated to analyze the kinematics in 2D of the horses at trot, we were able to correctly generate kinematics curves of the most important joints, and other angles of interest for veterinarians that are impossible to observe to the naked eye. In addition, we were able to recreate the gait or trot of the horses as a skeleton formed by articulated rigid bars. The trajectory graphs and the numerical results for angular variables (average angles, maximum, minimum, and angular motion range) were determined and simulated in 2D. The model generated allowed a qualitative and objective analysis of the equine movement (removing the subjectivity in assessing movement patterns), the control of rehabilitation and training programs, and the effective verification of the pharmacological or surgical treatments, among other factors.

The mathematical model of equine biokinematics can be used in two directions: one, by extracting the trajectories and the horse angular movement to understand and evaluate the kinematics of the joints, and two, by employing trajectories and joint angles in the field of robotics, in order to induce movements in quadruped robots to simulate the movement of electromechanical devices and quadruped animals. Graphic animations by computer are also useful for studying the morphology and movement of equines and other animals in the video game and movies industries, and in many other fields.

The numeric differences between the experimental and theoretical averages, and the average and standard deviation for the differences in every angular variable were small, except for the elbow and hip that presented a slightly greater variation. The reason for this may be that while in the mathematical model the lengths of the body segments are constant, in the experimental method these lengths are variable because they were calculated at every time sequence. The shape pattern of the graphs for the angular variables obtained by the model agrees with those previously reported in the literature for trotting horses.

Knowing how the major joints move in a horse is very useful for understanding the etiology, course, and treatment of injuries in tissues. Having a good mathematical model of horse motion will help future research on horse kinematics at different gaits, inclinations, speeds, breeds, surfaces, with real, simulated, or induced lameness, etc.

Acknowledgements

The authors thank PhD. Alfonso Martinez Galisteo, PhD. Juan Luis Garrido, and PhD. Rafael Medina Carnicer of the Department of Anatomy and Comparative Pathology - Faculty of Veterinary Medicine, University of Córdoba (Spain), for their support, advice and information on the kinematics of Andalusian horses at trot, information that was used to validate the functionality of the developed mathematical model. The authors acknowledge the support and advice at different stages of this study to the MSc and Zootechnician Veterinarian José Luis Velázquez Ramírez at the Faculty of Medicine and Veterinary, and Octavio Jiménez Espinoza, student of Mechanical Engineering at the National Autonomous University of Mexico. A special thanks is given to the scholarship program of the CEP -

UNAM for the financial support to complete the PhD studies that resulted in this paper. Also, thanks to the General Direction for Academic Personnel of UNAM (DGAPA-UNAM) for financial support provided through project IN113710 PAPIIT.

References

[1] A. Vukolov, A. Golovin, and N. Umnov, "Horse Gait Exploration on Step, Allure by Results of High Speed Strobe light Photography," in *Symposium a Quarterly Journal in Modern Foreign Literatures*, pp. 361-368, 2010.

[2] M. Valera, A. Molina, and F. Goyache, "Assessment of inbreeding depression for body measurements in Spanish Purebred (Andalusian) horses," *Livestock Science,* vol. 122, pp. 149-155, 2008.

[3] M. C. Hilary, and H. C. Schamhardt, "Measurement Techniques for Gait Analysis," in *Equine Locomotion*, Ed. W.B. Saunders, London, pp 55-76, 2000.

[4] I. D. Wijnberg, J. Sleutjens, J. H. Van Der Kolk, and W. Back, "Effect of head and neck position on outcome of quantitative neuromuscular diagnostic techniques in Warmblood riding horses directly following moderate exercise," *Equine Vet. J.,* vol. 42, pp. 261-267, Nov. 2010. DOI: http://doi.org/10.1111/j.2042-3306.2010.00224.x.

[5] C. Degueurce, H. Chateaua, V. Pasqui-Boutardb, P. Pourcelota, F. Audigiéa, N. Crevier-Denoixa, H. Jerbia, D. Geigerc, and J.-M. Denoix, "Concrete use of the joint coordinate system for the quantification of articular rotations in the digital joints of the horse," *Veterinary Research*, vol. 31 (3), pp. 297-311, May. 2000. DOI: http://doi.org/10.1051/vetres:2000102.

[6] L. Raghunandana, "*Development and validation of biomechanical models to quantify horseback forces at the walk in three horse breeds,"* Thesis (Master of Science in Electrical Engineering), Louisiana State University, Department of Electrical and Computer Engineering, 2011.

[7] V. D. Bogert, H. C. Schamhardt, and A. Crowe, "Simulation of quadrupedal locomotion using a rigid body model," *J. Biomech*., vol. 22 (1), pp. 33-41, Jan. 1989. DOI: http://doi.org/10.1016/0021-9290(89)90182-6.

[8] M. De Souza, "Influence of camped under associated with upright pastern in front conformation in the forelimb movement of horses," *J. of Equine Vet. Sci.*, vol. 24 (8), pp. 341-346, Aug. 2004. DOI: http://doi.org/10.1016/j.jevs.2004.07.005.

[9] A. Galisteo, and R. Vivo, "Patrón locomotor del trote del caballo Pura Raza Español y su variabilidad," *RECVET- Revista Electrónica de Clínica Veterinaria*, vol. III, pp. 1-17, 2008.

[10] A. Molina, M. Valera, A.M. Galisteo, J. Vivo, M.D. Gómez, A. Rodero, and E. Agüera, "Genetic parameters of biokinematic variables at walk in the Spanish Purebred (Andalusian) horse using experimental treadmill records," *Livestock Science*, vol. 116 (1-3), pp. 137-145, Jul. 2008. DOI: http://doi.org/10.1016/j.livsci.2007.09.021.

[11] M. R. Cano, J. Vivo, F. Miró, J. L. Morales, and A. M. Galisteo, "Kinematic characteristics of Andalusian, Arabian and Anglo-Arabian horses: a comparative study," *Res. Vet. Sci.,* vol. 71 (2), pp. 147-153, Oct. 2001. DOI: http://doi.org/10.1053/rvsc.2001.0504.

[12] H. M. Clayton, "Comparison of the stride kinematics of the collected, working, medium and extended trot in horses," *Equine Vet. J.,* vol. 26 (3), pp. 230-234, May. 1994. DOI: http://doi.org/10.1111/j.2042-3306.1994.tb04375.x.

[13] A. M. Galisteo, M. R. Cano, J. L. Morales, J. Vivo, and F. Miró, "The influence of speed and height at the withers on the kinematics of sound horses at the hand-led trot," *Vet. Res. Commun.*, vol. 22 (6), pp. 415-423, 1998. DOI: http://doi.org/10.1023/A:1006105614177.

[14] E. Barrey, B. Landjerit, and R. Wolter, "Shock and Vibration during the hoof impact on different track surfaces," *Equine Exerc. Physiol.*, no. 3, pp. 97-106, 1991.

[15] H. M. Clayton, D. H. Sha, J. A. Stick, and P. Robinson, "3D kinematics of the interphalangeal joints in the forelimb of walking and trotting horses," *Vet. Comp. Orthop. Traumatol.,* vol. 20 (1), pp. 1-7, 2007.

[16] H. M. Clayton, D. Sha, J. Stick, and N. Elvin, "3D kinematics of the equine metacarpophalangeal joint at walk and trot," *Vet. Comp. Orthop. Traumatol.*, vol. 20 (2), pp. 86-91, 2007. DOI: http://doi.org/10.1160/vcot-07-01-0011.

[17] Y. Torres-Pérez, E. Y. Gómez-Pachón, F. Cuenca-Jiménez, "Horse's gait motion analysis based on videometry," *Rev. Cien. Agri.,* vol. 13 (2), pp. 83-94, 2016.

[18] Y. Torres-Pérez, F. Cuenca, and A. Ortiz, "*Cinemática articular 2D de un caballo durante marcha normal,"* SOMIM, pp. 948-956, 2011.

[19] Y. Torres-Pérez, O. Jiménez, and A. Ortiz, "Generated Graphical Interface Design of the Normality Bands of the 2D Equine Kinematics," *Revista Argentina de Bioingeniería*. vol. 20, no. (1), pp. 39-42, 2014.

[20] F. Miró, J. Vivo, R. Cano, A. Diz, and A. M. Galisteo, "Walk and trot in the horse at driving: kinematic adaptation of its natural gaits," *Anim. Res.,* vol. 55 (6), pp. 603-613, Nov. 2006. DOI: http://doi.org/10.1051/animres:2006038.

[21] R. C. Hibbler, "*Dinámica – Mecánica para ingeniería,"* Prentice Hall, Ciudad de México, 2004.

[22] M.J.D. Powell, "A method for minimizing a sum of squares of non-linear functions without calculating derivatives," *Comput. J.,* vol. 7 (4), pp. 303-307, 1965. DOI: http://doi.org/10.1093/comjnl/7.4.303.

[23] R. Fletcher, "Function minimization without evaluating derivatives a review," *Comput. J.,* vol. 8 (1), pp. 33-41, 1965. DOI: http://doi.org/10.1093/comjnl/8.1.33.

[24] A. Byström, M. Rhodin, K. Peinen, M. A. Weishaupt, and L. Roepstor, "Basic kinematics of the saddle and rider in high-level dressage horses trotting on a treadmill," *Equine Vet. J.,* vol. 41 (3), pp. 280-284, Mar. 2009. DOI: http://doi.org/10.2746/042516409X394454.

[25] A. Veinguertener, T. Hoinville, O. Bruneau, and J. Fontaine, "Two-Legged Animals to the HexaQuaBip Robots Reconfigurable Kinematics," in *ICIRA*, pp. 1255-1265, 2009.

[26] C. Y. Li, H. T. Gao, Y. B. Ma, C. Liu, and H. Wang, "Artificial Horse for Rehabilitation," *Springer-Verlag Berlin Heidelberg,* no. 19, pp. 497-499, 2008. DOI: http://doi.org/10.1007/978-3-540-79039-6_124.

[27] M. Walter, and C. G. Franco, "Fast Customization of Geometric Models," *IEEE*, pp. 146-151, 2000. DOI: http://doi.org/10.1109/sibgra.2000.883907.

[28] L. Reveret, L. Favreau, C. Depraz, and M. P. Cani, "Morphable model of quadrupeds skeletons for animating 3D animals," in *Symposium on Computer Animation*, pp. 135-142, 2005. DOI: http://doi.org/10.1145/1073368.1073386.

[29] E. Boxerman, *Dynamic Model of a Horse Gallop in 2D,* Available at: http://www.cs.ubc.ca/~eddybox/projects/533B/.

[30] L. Skrba, L. Reveret, F. Hétroy, M.-P. Cani, and C. O'Sullivan, "Animating Quadrupeds: Methods and Applications," *Computer Graphics Forum,* vol. 28 (6), pp. 1541-1560, Sep. 2009. DOI: http://doi.org/10.1111/j.1467-8659.2008.01312.x.

[31] A. M. Galisteo, M. R. Cano, J. L. Morales, F. Miró, J. Vivo, and E. Agüera, "Kinematics in horses at the trot before and after an induced forelimb supporting lameness," *Equine Vet. J. Suppl.,* vol. 29 (S23), pp. 97-101, 1997. DOI: http://doi.org/10.1111/j.2042-3306.1997.tb05064.x.